

Thiophene-Fused Ladder Boroles with High Antiaromaticity

Azusa Iida and Shigehiro Yamaguchi*

Department of Chemistry, Graduate School of Science, Nagoya University and JST-CREST, Furo, Chikusa, Nagoya 464-8602, Japan

Supporting Information

ABSTRACT: A series of polycyclic thiophene-fused boroles were synthesized on the basis of stepwise substitution reactions from thienylboronic ester precursors. In these ladder-type π -conjugated systems, the thiophene-fused structure enhances the antiaromaticity of the borole ring. This trend is opposite to the conventional understanding that the arene-fused structure decreases the antiaromaticity of the 4π -electron ring skeletons. The ladder boroles exhibited characteristic properties such as long-wavelength absorptions and low reduction potentials.

Borole is isoelectronic to a 4π -electron cyclopentadienyl cation and thus represents an important building unit to investigate π -conjugated systems with antiaromatic characteristics.^{1,2} Theoretical studies have suggested unusual electronic features of borole-based π -conjugated systems.³ Whereas the first borole derivative, 1,2,3,4,5-pentaphenylborole, was reported by Eisch and co-workers in 1969,^{4,5} only recently has its crystal structure been determined by X-ray crystallography.^{6,7} Since then, significant attention has been focused on this chemistry. During the past few years, various fascinating borole derivatives have been developed,^{8,9} such as borole–metal complexes,^{8b} carbene-coordinated boroles,^{8c} and highly Lewis acidic boroles.⁹

One crucial issue in the molecular design of new borole-based materials is how to stabilize the borole skeleton. General strategies are to construct the ring-fused structure in order to decrease the antiaromaticity and to introduce a bulky aryl group onto the boron atom for kinetic stabilization (Figure 1). On the basis of these considerations, several stable dibenzoboroles **1** with potential utilities for various applications, such as fluorescent sensors^{10a} and electron-transporting materials,^{10b} were synthesized. However, examples of the ring-fused ladder-type borole derivatives are still limited, and their chemistry has not yet matured. In particular, little is known about heteroarene-fused borole derivatives.¹¹ It can be envisioned that fusing of the heteroarene rings, such as the electron-donating thiophene, should significantly perturb the electronic structure of the electron-accepting borole skeleton.

We now report synthetic methodologies for a series of thiophene-fused ladder boroles **2–4** and their unusual antiaromatic characteristics compared to the dibenzoborole **1a** ($R = iPr$, $Ar = H$) or the parent borole **5**. Recently, analogous ladder heteroles with various main-group elements,¹² such as compounds **6–8** containing Si,¹³ P,¹⁴ and S,¹⁵ have been reported as promising emitting materials and stable transistor materials. Comparisons with these other heteroles in terms of photophysical and electrochemical properties will also provide a clear-cut view of the uniqueness of the ladder boroles.

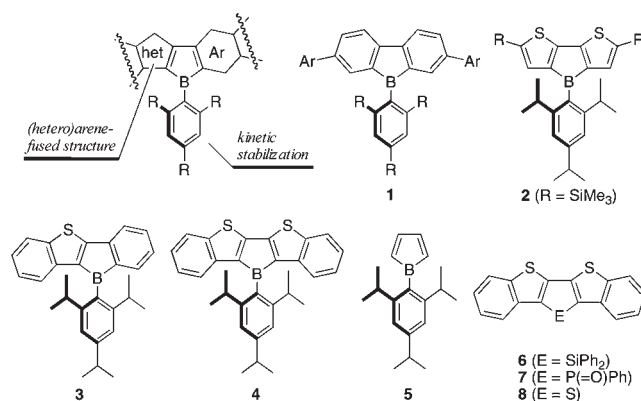
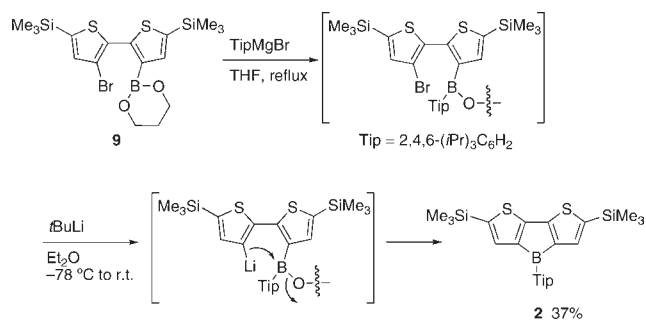


Figure 1. Ladder boroles and related compounds.

Scheme 1. Synthesis of Dithienoborole



The most straightforward synthetic route to the dithienoborole skeleton may be the reaction of dimetalated bithiophene with $ArBX_2$.¹¹ However, all our attempts were unsuccessful. Therefore, we explored an alternative route, stepwise substitution reactions on the boron atom, as shown in Scheme 1. Thus, using 3'-bromo-2,2'-bithienyl-3-boronic ester **9** as a key precursor, the 2,4,6-triisopropylphenyl (Tip) group was first introduced onto the boron atom by the reaction with TipMgBr in refluxing THF. As the Tip group is bulky enough to protect the boron center, lithiation with *t*BuLi then proceeded selectively at the 3' position of the bithiophene skeleton. The generated anion subsequently underwent intramolecular nucleophilic substitution on the boron atom to produce the target compound **2**. After silica gel column chromatography under an argon atmosphere, recrystallization from pentane gave the target compound in 37% yield.

Received: March 4, 2011

Published: April 19, 2011

Scheme 2. Synthesis of Ladder Boroles

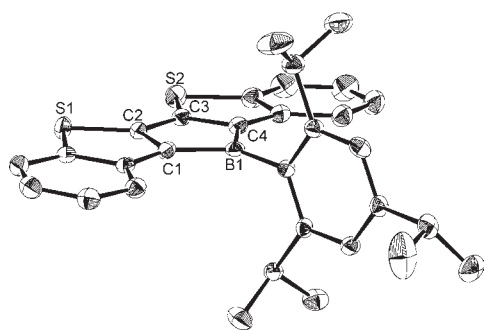
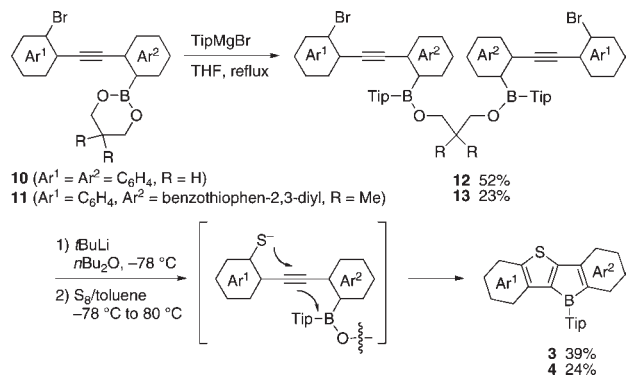


Figure 2. ORTEP drawing of **4** (50% probability for thermal ellipsoids). Hydrogen atoms are omitted for clarity.

The combination of the present stepwise substitution reaction with a domino-type intramolecular double cyclization¹⁶ enabled us to synthesize more extended ladder boroles, as shown in Scheme 2. The diarylacetylenes **10** and **11** bearing boronic ester groups were employed as precursors. Reactions of these compounds with TipMgBr selectively produced the corresponding dimeric products **12** and **13**, which were isolated by column chromatography in 52% and 23% yields, respectively. Successive treatments of these compounds with *t*BuLi and a toluene solution of elemental sulfur produced the thiolate anion intermediates, which underwent *5-endo-dig* cyclization followed by the intramolecular substitution at the boron atom. Overall, the borole and thiophene ring skeletons were constructed in a fused fashion in one step. Based on this procedure, a four-ring-fused borole **3** and a five-ring-fused borole **4** were obtained in 39% and 24% yields, respectively.

The products were identified by various NMR spectroscopies and mass spectrometry. In the ¹¹B NMR spectra, broad signals were observed at 62–65 ppm for **2–4**, which are characteristic of a borole boron atom.^{6,7} The structures of all the compounds were finally confirmed by X-ray crystallographic analysis (see the Supporting Information). As a representative example, an ORTEP drawing of the longest ladder borole **4** is shown in Figure 2.

Compound **4** has a nearly coplanar π -conjugated framework with small dihedral angles between the central borole and two terminal benzene rings of 2.00(14)° and 4.25(15)°. The Tip group is arranged perpendicular to the borole ring. As for the geometry of the borole ring, the B–C bond lengths (1.574(3) and 1.576(3) Å) and the C–B–C bond angle (102.84(15)°) are

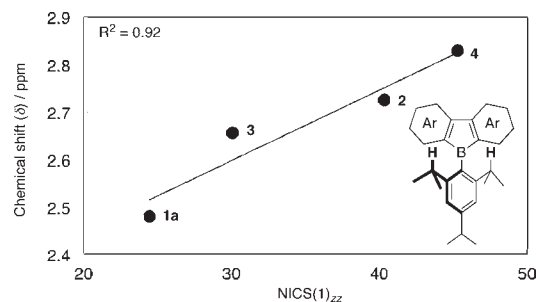


Figure 3. Plot of the ¹H NMR chemical shifts of the *ortho*-*i*Pr methyne protons for **1a–4** as a function of the NICS(1)_{zz} values of their borole rings. The calculations were conducted at the B3LYP/6-311+G** level.

comparable to those of the non-fused tetraphenylated borole derivatives.⁷ Worth noting is the extent of the bond alternation in the butadiene moiety. While the C1–C2 and C3–C4 bond lengths are 1.377(3) and 1.376(3) Å, respectively, the C2–C3 bond length is 1.478(3) Å. The extent of this bond alternation is rather small compared to those of the non-fused borole derivatives⁷ and also that of the parent borole **5** optimized at the B3LYP/6-31G* level. The small bond alternation in the borole ring is also observed for the other ladder compounds **2** and **3**. This structural feature should affect their electronic structures (*vide infra*).

We initially envisioned that the electron-donating thiophene would decrease the Lewis acidity of the boron atom and thereby stabilize the borole ring. Against our expectation, however, all the thiophene-fused ladder molecules were air- and moisture-sensitive and, therefore, needed handling under an argon atmosphere using dry solvents for purification. This is in contrast to the fact that the dibenzoborole **1a** can be isolated by silica gel column chromatography in the open atmosphere. This difference demonstrates the higher reactivity of the thiophene-fused borole skeletons. To elucidate this difference, we investigated the effect of the fused thiophene ring on the antiaromaticity of the borole ring. As a measure of the antiaromaticity, we evaluated the nucleus-independent chemical shift (NICS) values by the DFT calculations at the B3LYP/6-311+G** level,¹⁷ using the geometries derived from the crystal structures.¹⁸ All the thiophene-fused boroles have more positive NICS(1)_{zz} values than that (+29.4 ppm) of the parent borole **5**. This is in contrast to the fact that the dibenzoborole **1a** (+24.5) has a less positive NICS(1)_{zz} value than **5**. The NICS(1)_{zz} values increase in the order of **3** (+30.1) < **2** (+40.3) < **4** (+45.3).¹⁹

The trend in the antiaromaticity for the ladder boroles is consistent with the experimental observations. According to the crystal structures of the ladder boroles **1a–4**, the methyne protons of the *ortho*-isopropyl groups in the Tip group locate above and below the borole boron atom. In the ¹H NMR spectra, the chemical shifts of the methyne protons should be perturbed by the paratropic ring-current effects of the borole ring. Indeed, the chemical shifts of the methyne protons exhibited downfield shifts in the order of **1a** < **3** < **2** < **4**; more importantly, the plot of the δ values versus the calculated NICS(1)_{zz} values showed a linear relationship (Figure 3). All these results imply that the thiophene-fused structure enhances the antiaromaticity of the borole ring. Notably, this is opposite to the conventional understanding that fusion of the aromatic arene rings can decrease the antiaromatic character of the 4π electron skeletons.²⁰

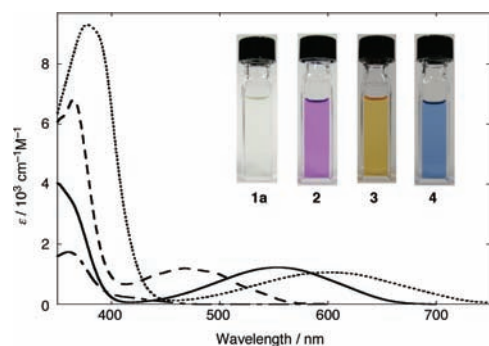


Figure 4. UV–vis absorption spectra of **2** (solid line), **3** (dashed line), and **4** (dotted line) in CH_2Cl_2 , together with that of **1a** (dashed dotted line). Inset: photographs of the CH_2Cl_2 solutions of **1a–4**.

Table 1. Photophysical and Electrochemical Data for the Ladder Boroles and Related Compounds

compd	UV–vis absorption ^a		reduction potential ^b	
	$\lambda_{\text{abs}}/\text{nm}$	$\log \epsilon$	$E_{1/2}/\text{V}^c$	E_{pc}/V^d
1a	420 (sh)	2.33	−2.11	−3.05
2	552	3.05	−1.98	−2.79
3	469	2.93	−1.96	−2.89
4	600	3.04	−1.72	−2.61

^a In CH_2Cl_2 . ^b Determined by cyclic voltammetry under the following conditions: sample 1 mM; $\text{Bu}_4\text{N}^+\text{PF}_6^-$ (0.1 M) in THF; scan rate 100 mVs^{-1} . ^c First reduction potential vs Fc/Fc^+ . ^d Second reduction peak potential vs Fc/Fc^+ .

This unusual effect of the thiophene-fused structure may be rationalized by considering the geometrical features of the thiophene-fused borole skeletons. We conducted NICS calculations on the parent boroles **5'** and **5''**, whose geometries were directly derived from the crystal structures of **2** and **4**, respectively, without including the thiophene moieties (see the Supporting Information). Notably, these boroles have much more positive NICS(1)_{zz} values, +43.3 and +40.3 ppm, than that of the optimized **5**, despite the absence of an electronic influence from the thiophene rings. These results suggest that the borole geometry in the thiophene-fused skeleton should be the origin of the enhanced antiaromaticity. A major difference in the geometries between the boroles **5'** and **5''** and the optimized **5** is the extent of bond alternation. While in general the borole ring tends to have a large bond alternation in the butadiene moiety in order to minimize the antiaromatic character,⁷ the butadiene moieties in **5'** and **5''** have shorter C–C single bonds as well as longer C=C double bonds compared to those in **5**, resulting in the smaller extent of the bond alternation, as described in the crystal structure section. This may be responsible for the enhanced antiaromaticity of the thiophene-fused borole skeletons.

We have two interests regarding the electronic properties. One is how the thiophene-fused structure affects the photophysical and electrochemical properties compared to the benzene-fused structure. The other is how the ladder boroles are different from the other ladder heteroles. In the UV–vis absorption spectra in CH_2Cl_2 , the thiophene-fused ladder boroles indeed showed characteristic absorption bands, as shown in Figure 4. Their data are summarized in Table 1. While the dibenzoborole **1a** showed the

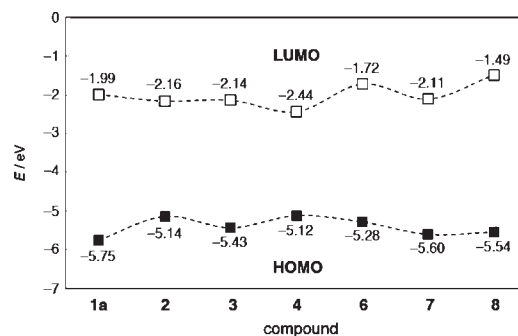


Figure 5. Kohn–Sham HOMO and LUMO energy levels for a series of the ladder boroles **1a–4** and related compounds **6–8**, calculated at the B3LYP/6-31G* level of theory.

longest absorption maximum (λ_{max}) at 420 nm as a weak shoulder band, the dithieno-fused analogue **2** showed a purple color, and its longest λ_{max} was 552 nm, which is more than 130 nm red-shifted compared to that of **1a**. The molar absorption coefficient was also increased by replacing the benzene ring with a thiophene ring. Notably, the four-ring-fused **3** has a shorter λ_{max} than **2**, despite its longer π -conjugated framework, indicative of the unique electronic structure of the “dithieno-fused” borole skeleton. In fact, the more extended ladder molecule **4**, with the dithienoborole skeleton, has the longest λ_{max} of 600 nm and showed a blue color. It is noteworthy that this λ_{max} value is much longer even compared to those of the other heterole analogues with identical π -conjugated lengths: **6**, 382 nm;¹³ **7**, 424 nm;¹⁴ **8**, 344 nm.^{15b}

In the fluorescence spectra, while the dibenzoborole **1a** showed a green fluorescence at 522 nm with a quantum yield of 0.48 (CH_2Cl_2), all the thiophene-fused boroles **2–4** were non-emissive. This difference suggests the different nature of the excited states between **1a** and **2–4**.

To gain insight into the electronic structures of the ladder boroles, we compared the frontier orbital energy levels of **1a–4** and **6–8**, as shown in Figure 5. There are some notable points. (1) While the dithieno-fused borole **2** has a slightly lower-lying LUMO than that of the dibenzo-fused analogue **1a**, the HOMO of **2** is substantially higher, by 0.61 eV, compared to that of **1a**. This difference in the HOMO level mainly contributes to the significantly red-shifted λ_{max} of the dithienoborole. (2) Whereas the antiaromaticity increases in the order of **1a** < **3** < **2** (*vide supra*), the LUMO levels of **2** and **3** are lower than that of **1a** but are comparable to each other. This comparison implies that the LUMO level and antiaromaticity are not directly related. (3) Among a series of bis(benzothieno)heteroles, the ladder borole **4** has the lowest-lying LUMO. While incorporation of the electron-withdrawing P=O moiety is recognized as an effective strategy to attain a low LUMO level,^{14,21} this also results in a decreased HOMO level. In contrast, incorporation of the boron atom decreases the LUMO level while maintaining the high HOMO level. The lower LUMO level of **4** compared to the P=O-containing **7** demonstrates the significant effect of the orbital interaction in the borole ring. As a consequence, **4** has the longest λ_{max} among the series of bis(benzothieno)heteroles. Time-dependent DFT calculations confirmed that the major contributions to the longest absorption band for all these compounds are the HOMO–LUMO transitions.

To experimentally confirm the electronic features discussed in the previous section, we measured the cyclic voltammetry

for **1a–4**. Their electrochemical data are also summarized in Table 1. All the ladder boroles showed two-step reduction processes with the first reversible redox waves and the second irreversible reduction wave. Notably, the first reduction potential of **4** ($E_{1/2} = -1.72$ V vs Fc/Fc⁺) is more positive than that of the P=O-containing analogue **7** ($E_{1/2} = -1.98$ V vs Fc/Fc⁺).²² This difference demonstrates the uniqueness of the borole ring as an electron-accepting building unit.

In summary, we established a synthetic route to the thiophene-fused ladder boroles based on the stepwise substitution of the thienylboronic esters. The boroles **2–4** are air- and moisture-sensitive due to the enhanced antiaromaticity of the borole ring with the thiophene-fused skeleton. The characteristic absorption and electrochemical properties of the ladder boroles, significantly different from those of the other known heterole analogues, demonstrate the uniqueness of the borole skeleton as a building unit. These results provide important fundamental knowledge on the extended π -electron systems with high antiaromatic characteristics. Further study on the structure–properties relationships for a variety of heteroarene-fused boroles is now in progress.

■ ASSOCIATED CONTENT

S Supporting Information. Experimental procedures and spectral data for all new compounds, crystallographic data and ORTEP drawings of **1a–4**, and results of theoretical calculations. This material is available free of charge via the Internet at <http://pubs.acs.org>.

■ AUTHOR INFORMATION

Corresponding Author

yamaguchi.shigehiro@b.mbox.nagoya-u.ac.jp

■ ACKNOWLEDGMENT

This work was partly supported by a Grant-in-Aid (No. 19675001) from the Ministry of Education, Culture, Sports, Science, and Technology, Japan, and CREST, JST. A.I. acknowledges the JSPS research fellowship for young scientists.

■ REFERENCES

- (1) Huynh, K.; Vignolle, J.; Tilley, T. D. *Angew. Chem. Int. Ed.* **2009**, *48*, 2835.
- (2) (a) Minsky, A.; Meyer, A. Y.; Rabinovitz, M. *Tetrahedron* **1985**, *41*, 785. (b) Jusélius, J.; Sundholm, D. *Phys. Chem. Chem. Phys.* **2008**, *10*, 6630.
- (3) (a) Salzner, U.; Lagowski, J. B.; Pickup, P. G.; Poirier, R. A. *Synth. Met.* **1998**, *96*, 177. (b) Cao, H.; Ma, J.; Zhang, G.; Jiang, Y. *Macromolecules* **2005**, *38*, 1123.
- (4) Eisch, J. J.; Hota, N. K.; Kozima, S. *J. Am. Chem. Soc.* **1969**, *91*, 4575.
- (5) (a) Eisch, J. J.; Galle, J. E.; Kozima, S. *J. Am. Chem. Soc.* **1986**, *108*, 379. (b) Eisch, J. J.; Galle, J. E.; Shafii, B.; Rheingold, A. L. *Organometallics* **1990**, *9*, 2342. (c) Fagan, P. J.; Nugent, W. A.; Calabrese, J. C. *J. Am. Chem. Soc.* **1994**, *116*, 1880.
- (6) Braunschweig, H.; Fernández, I.; Frenking, G.; Kupfer, T. *Angew. Chem. Int. Ed.* **2008**, *47*, 1951.
- (7) So, C.-W.; Watanabe, D.; Wakamiya, A.; Yamaguchi, S. *Organometallics* **2008**, *27*, 3496.
- (8) (a) Braunschweig, H.; Kupfer, T. *Chem. Commun.* **2008**, 4487. (b) Braunschweig, H.; Chiu, C.-W.; Radacki, K.; Brenner, P. *Chem. Commun.* **2010**, *46*, 916. (c) Braunschweig, H.; Chiu, C.-W.; Radacki, K.; Kupfer, T. *Angew. Chem. Int. Ed.* **2010**, *49*, 2041. (d) Braunschweig, H.;

Breher, F.; Chiu, C.-W.; Gamon, D.; Nied, D.; Radacki, K. *Angew. Chem. Int. Ed.* **2010**, *49*, 8975.

(9) (a) Fan, C.; Piers, W. E.; Parvez, M. *Angew. Chem. Int. Ed.* **2009**, *48*, 2955. (b) Fan, C.; Mercier, L. G.; Piers, W. E.; Tuononen, H. M.; Parvez, M. *J. Am. Chem. Soc.* **2010**, *132*, 9604. (c) Fan, C.; Piers, W. E.; Parvez, M.; McDonald, R. *Organometallics* **2010**, *29*, S132.

(10) (a) Yamaguchi, S.; Shirasaka, T.; Akiyama, S.; Tamao, K. *J. Am. Chem. Soc.* **2002**, *124*, 8816. (b) Wakamiya, A.; Mishima, K.; Ekawa, K.; Yamaguchi, S. *Chem. Commun.* **2008**, 579.

(11) The synthesis of a dithienoborole derivative was reported previously, but its photophysical properties are largely different from our results: Kim, S.; Song, K.; Kang, S. O.; Ko, J. *Chem. Commun.* **2004**, 68.

(12) Fukazawa, A.; Yamaguchi, S. *Chem. Asian J.* **2009**, *4*, 1386.

(13) Ohshita, J.; Lee, K.-H.; Kimura, K.; Kunai, A. *Organometallics* **2004**, *23*, S622.

(14) Dienes, Y.; Eggenstein, M.; Kárpáti, T.; Sutherland, T. C.; Nyulászi, L.; Baumgartner, T. *Chem. Eur. J.* **2008**, *14*, 9878.

(15) (a) Schroth, W.; Hintzsche, E.; Viola, H.; Winkler, R.; Klose, H.; Boese, R.; Kempe, R.; Sieler, J. *Chem. Ber.* **1994**, *127*, 401. (b) Okamoto, T.; Kudoh, K.; Wakamiya, A.; Yamaguchi, S. *Org. Lett.* **2005**, *7*, 5301. (c) Gao, J.; Li, R.; Li, L.; Meng, Q.; Jiang, H.; Li, H.; Hu, W. *Adv. Mater.* **2007**, *19*, 3008.

(16) Mouri, K.; Wakamiya, A.; Yamada, H.; Kajiwara, T.; Yamaguchi, S. *Org. Lett.* **2007**, *9*, 93.

(17) (a) Schleyer, P. v. R.; Maerker, C.; Dransfeld, A.; Jiao, H.; van Eikema Hommes, N. J. R. *J. Am. Chem. Soc.* **1996**, *118*, 6317. (b) Corminboeuf, C.; Heine, T.; Seifert, G.; Schleyer, P. v. R.; Weber, J. *Phys. Chem. Chem. Phys.* **2004**, *6*, 273. (c) Fallah-Bagher-Shaldael, H.; Wannere, C. S.; Corminboeuf, C.; Puchta, R.; Schleyer, P. v. R. *Org. Lett.* **2006**, *8*, 863.

(18) The NICS values based on the optimized structures for the corresponding model compounds were also consistent with the values obtained for the crystal structures (Supporting Information).

(19) The NICS(1)_{zz} values of the thiophene rings in **2**, **3**, and **4** are -13.1 , -12.3 , and -13.7 ppm, respectively.

(20) Allen, A. D.; Tidwell, T. T. *Chem. Rev.* **2001**, *101*, 1333.

(21) (a) Baumgartner, T.; Réau, R. *Chem. Rev.* **2006**, *106*, 4681. (b) Fukazawa, A.; Hara, M.; Okamoto, T.; Son, E.-C.; Xu, C.; Tamao, K.; Yamaguchi, S. *Org. Lett.* **2008**, *10*, 913.

(22) This value was determined under conditions identical with those for the measurement of **4** and is consistent with the value originally reported in the literature ($E_{1/2} = -1.45$ V vs Ag/AgCl).¹⁴